S.E. Beaubien,*, G. Ciotoli, P. Coombs, M.C. Dictorc, M. Kruger, S. Lombardi, J.M. Pearce, J.M. West

The impact of a naturally occurring CO2 gas vent on the shallow ecosystem and soil chemistry of a Mediterranean pasture (Latera, Italy)

Recent research into CO2 geological storage has shown that it has potential to be a safe and effective way to rapidly decrease short-term anthropogenic CO2 emissions. Despite this progress, stakeholders must be convinced that the scientific community has studied all possible scenarios, including a potential leak into the biosphere. To better understand the potential impact of such an event, a detailed geochemical and biological study was conducted during two different seasons on a naturally occurring gas vent located within a Mediterranean pasture ecosystem (Latera geothermal field, central Italy). Results from botanical, soil gas, and gas flux surveys, and from chemical and biological analyses of shallow soil samples (0–20 cm depth), show that a significant impact is only observed in the 6 m wide centre of the vent, where CO2 flux rates exceed 2000–3000 g m□2d□1. In this ‘‘vent core’’ there is no vegetation, pH is low (minimum 3.5), and small changes are observed in mineralogy and bulk chemistry. In addition, microbial activities and populations are regulated in this interval by near-anoxic conditions, and by elevated soil gas CO2 (>95%) and trace reduced gases (CH4,H2S, and H2). An approximately 20 m wide halo surrounding the core forms a transition zone, over which there is a gradual decrease in CO2 concentrations, a rapid decrease in CO2 fluxes, and the absence of reactive gas species. In this transition zone grasses dominate near the vent core, but these are progressively replaced by clover and a greater plant diversity moving away from the vent centre. Physical parameters (e.g. pH, bulk chemistry, mineralogy) and microbial systems also gradually return to background values across this transition zone. Results indicate that, even at this anomalous high-flux site, the effects of the gas vent are spatially limited and that the ecosystem appears to have adapted to the different conditions through species substitution or adaptation.

Introduction: average global temperatures observed over the last century is
likely due to the release of anthropogenic greenhouse gases. The recently released fourth IPCC report on global warming Of particular concern in this report are modelling results that (IPCC, 2007) states with ever-more certainty that the rise in predict that the global climate system will continue to change towards a new equilibrium for hundreds of years, even considering a reduction of human emissions over the next 50–100 years. As a result, it is clear that large-scale solutions are needed immediately which have the potential to quickly reduce emissions, while at the same time allowing for continued economic growth and the development of alternative energy sources.

Carbon dioxide capture from fixed sources, such as fossil fuel burning power plants, and its storage in porous geological formations is one such technique which holds great promise. This technology exists today, based on experience gained over the last 50 years via enhanced oil recovery operations (Worden and Smith, 2004), natural gas storage (Gumrah et al., 2005), and acid gas injection (Bachu and Gunter, 2004). Large research projects have examined CO2 capture, transport, and storage capacity (e.g. Holloway, 1996), and issues related to the evolution, stability and safety of CO2 geological storage reservoirs have been studied in great detail at industrial sites like Weyburn (Wilson and Monea, 2004) and Sleipner (Chadwick et al., 2006). The extensive work conducted at these last two sites has shown how a well-chosen and properly engineered site can both isolate large volumes of CO2 for long periods of time and be intrinsically safe.

In order to proceed with the large-scale deployment of this technique, however, a well-developed regulatory environment needs to be put in place, and for this to happen it is paramount that governments and the public at large are well informed and are convinced that all potential risks have been studied and determined to be sufficiently small. While it is obvious that this includes the integrity of the reservoir itself to contain the CO2, it is equally important to also assess the potential risks associated with the unlikely leakage of significant volumes of CO2 from the reservoir into the near surface environment (West et al., 2005, 2006).

Although numerous studies have been published regarding the effect of increasing atmospheric CO2 concentrations on ecosystems (e.g. Jossi et al., 2006), there are far fewer that have examined the effects of increasing CO2 concentrations in the soil horizon due to upwardly migrating gas. Typically these latter studies involve the use of natural test sites where deep-origin, natural CO2 is released to the atmosphere. Examples include the study of a site near Stavesinci (NE Slovenia) for the influence of high soil-gas concentrations of geothermal-origin CO2 on grass health and root respiration (Macek et al., 2005; Pfanz et al., 2007; Vodnik et al., 2006) and Mammoth Mountain (CA, USA) for the influence of magmatic CO2 on soil chemistry and mineralogy (Stephens and Hering, 2002, 2004)and tree mortality(Biondi and Fessenden, 1999).

A number of other studies have also been conducted to examine long-term ecosystem responses to elevated atmospheric CO2 concentrations induced by nearby natural CO2 vents and springs, such as at Hakanoa Springs, New Zealand (Kool et al., 2007; Rillig et al., 2000; Ross et al., 2000), Olafsvik, W. Iceland (Cook et al., 1998), and Pleasant View Farm, South Africa (Stock et al., 2005). Unfortunately these works only report time-averaged atmospheric CO2 concentrations, and thus it is difficult to understand if the observed effects were also influenced by high concentrations of un-measured or un-reported root zone CO2.

The present paper also studies a natural test site (Latera, Italy; Fig. 1a) where deep geothermal CO2 is released to the atmosphere from a venting structure. Here a 50 m long transect was performed across this vent, with continuous botanical measurements and detailed soil gas sampling used to define zones for subsequent soil sampling. The goal of this work was then to integrate the botanical and soil gas results with various geochemical, biological, and microbial measurements conducted on the soil samples to better understand the potential impact of CO2 leaking from a geological storage reservoir on the shallow ecosystem.

2. Geology and site description

The Latera caldera, located in west-central Italy, is a large, elliptical (10 km □ 8 km), NNE-SSW trending structure with several eruptive vents located both within and outside of the caldera. Now inactive for over 0.16 Ma (Vezzoli et al., 1987), this volcanic structure still has an extremely high geothermal gradient, and it is believed that associated thermo-metamorphic reactions in carbonate rocks are the source of the large quantities of deep CO2 and other trace gases that are released to the atmosphere from various discrete gas vents throughout the valley (Duchi et al., 1992). A detailed treatment of the geology and structure of the Latera caldera, as well as a discussion of gas migration along faults in the area, is given by Annunziatellis et al. (2008).

Surface lithology throughout the caldera floor is dominated by alluvial sediments, while the overlying soils are highly fertile due to formation from the alkali-potassic units of the Latera volcanic complex. The study site itself is found in the centre of the caldera (Fig. 1a) within a small, essentially flat field that is used for sheep pasture. The soil in this field is not tilled but rather the natural vegetation, primarily clover and grass, is harvested twice a year for animal feed. The local climate is Mediterranean, with hot dry summers and cool wet winters.

The studied field contains a number of gas vents, however the present work is restricted to one (gas vent ‘‘A’’; GVA) that is isolated and well-defined, and which has been extensively characterised using various geochemical (Annunziatellis et al., 2008; Lombardi et al., 2006; Pearce, 2004), geophysical (Pettinelli et al., 2004, 2008), and remote sensing (Bateson et al., 2008) tools. This feature, which releases approximately 200 kg of CO2 to the atmosphere per day (Beaubien, unpublished data), is thought to be located at thegas permeablejunctureoftwo faults (Annunziatellis et al., 2008).

The vent consists of a 6 m diameter non-vegetated core surrounded by an 18 m wide transition zone where impact on vegetation progressively decreases as the soil approaches background conditions (Fig.

1b). Within the vent core there are high CO_2 flux rates, as well as nearly 100% CO_2 plus other trace gases such as CH_4, H_2S and H_2 in the soil horizon. Within the transition zone CO_2 flux rates decrease markedly, CO_2 soil gas concentrations decrease gradually, and reduced trace gases are not observed. As such, this transition zone provides an ideal opportunity to examine the effect of a wide range of CO_2 concentrations/fluxes within the same soil type without the complication of other gas species.

Although the age of this gas vent is not exactly known, interviews with local residents indicate that it has been active and stable for more than 75 years. Considering the high heat flow in the area there is the potential that the vent has been active for a much longer period, perhaps on the order of hundreds of years. As such the observed trends have likely formed after a long period of time and the chemical system is in a quasi-steady state. The biological system is expected to be more transient, due to meteorological and seasonal effects.

3. Methods

Two field campaigns were conducted during two different growing seasons, one in September of 2005 and the other in June of 2006. Measurements during both campaigns were performed along a 1 m wide, 50 m long transect that crossed all intervals impacted by the studied gas vent (Fig. 1b), providing a complete spectrum of CO_2 flux rates, CO_2 soil gas concentrations, and soil gas compositions.

Initial work involved a continuous botanical survey along the transect and detailed soil gas sampling (once every metre) to define the spatial distribution of CO_2 along the profile. This information was then used to select a total of 15 locations for subsequent soil sampling with a hand auger, with sites chosen to best represent the lateral variability of CO_2 concentrations. Some or all of these 15 samples were subsequently analysed for various chemical and biological parameters; this results in individual methods having different sample densities along the profile, as seen in the respective graphs discussed below.

3.1. Gas geochemistry

Soil gas samples were collected by pounding a stainless-steel probe (with a sacrificial tip) to the desired depth (10 and 20 cm) and drawing 60 ml of gas from the probe with a bulb pump or plastic syringe to remove any atmospheric air (Ciotoli et al., 1998, 1999). Soil gas was then analysed directly from the probe for CO_2, O_2, H_2S, and H_2 using infrared and electrochemical analysers (Geotechnical Instruments GA2000 or Draeger Multiwarn). 60 ml samples were also collected in 25 ml stainless-steel containers for laboratory analysis of helium on a Varian mass spectrometer and light hydrocarbons, CO_2, N_2, and O_2 + Ar on two Fisons 8000series bench gas chromatographs (GC). A dataset ($n = 30$) consisting of quality control analyses of known standards, conducted during sample analysis, was used to estimate the standard deviation (1s) of these GC measurements: $CH_4 = 2.2 \pm 0.1$ ppm; $CO_2 = 2.5 \pm 0.1\%$; O_2 + Ar = $20.4 \pm 0.5\%$; and $N_2 = 78.1 \pm 1.8\%$.

A limited number of CO_2 flux measurements were only made during the June 2006 campaign using a WestSystems LI820 CO_2 flux meter. Measurements involved the initial removal of surface vegetation, after which the accumulation chamber was pressed directly against the soil with sufficient force to provide a good seal. Chamber CO_2 concentration was monitored for 120 s and flux was calculated based on the rate of change, chamber parameters, and environmental conditions (e.g. Lewicki et al., 2005). Measurement repeatability of the accumulation chamber method has been estimated to be ±10% (Chiodini et al., 1998).

3.2. Soil sampling

Samples of soils and underlying sediments were collected using a hand-held auger. A total of 15 locations along the transect were chosen for soil sampling, based on the relative distribution of soil gas CO_2. Two samples were taken from each location: one from 0 to 20 cm (within the root zone) and a second from 50 to 70 cm (within the soil B-horizon). Note that only the root zone results are reported here.

To minimise cross contamination, all tools and gloves were cleaned with ‘disinfectant’ wipes, deionised water, alcohol, and then air dried prior to sampling and sub-sampling. Almost all soil samples were pre-sieved in the field to pass 2 mm and quickly homogenized to avoid drying of the samples (three could not be sieved within appropriate time limits imposed by microbial analyses because of their higher water and clay contents). Each homogenized sample was then sub-sampled for the various analyses described below. For most methods each sample was analysed only a single time, due to the large number of sampling points and methods used. Note that while biological analyses were conducted on soil samples collected from these locations during both field seasons, solid phase chemical analyses (like mineralogy, bulk chemistry, and trace elements) were performed only on those from the September 2005 season.

3.3. Mineralogy and other chemical analyses

For whole-rock X-ray diffraction (XRD) analysis ca. 3 g of milled sediment material was wet-micronised under acetone for 10 min, dried at 55 8C, disaggregated, and back-loaded onto standard stainless steel sample holders for analysis. A PANalytical X’Pert Pro series diffractometer was used, equipped with a cobalt-target tube, X’Celerator detector, and operated at 45 kV and 40 mA. Samples were scanned from 4.5 to 858 2u at 2.768 2u/min and analysed using 2004 PANalytical X’Pert Pro software coupled to the latest version of the International Centre for Diffraction Data (ICDD) database.

Approximately 50 g of dry material was weighed, resuspended with deionised water, and then wet sieved through a 0.063 mm sieve to obtain the silt and clay fraction. This fraction was then evenly split for clay-XRD and Sedigraph analysis. Clay-XRD measurements involved: dispersion of ca. 5 g of the <0.063 mm fraction in deionised water; removal of the <2 mm fraction after a period determined using Stokes’ Law; drying; creation of an oriented mount using 100 mg of material; Ca saturation using 2 ml 0.1 M CaCl2□6H2O solution; and eventual scanning from 2 to 328 2u at 0.548 2u/min as air-dry mounts, after glycol-solvation, and after heating to 550 8C for 2 h. Sedigraph analyses involved suspension of the <0.063 mm fraction in a 0.2% sodium hexametaphosphate solution (‘‘Calgon’’) and the analysis of particle size distribution over the size range from 0.0063 to 0.001 mm. A standard reference material was run before the samples to ensure the machine was operating correctly.

Cation exchange capacity (CEC) was measured by saturating samples with barium (supplied as a 1:1 barium chloride/triethanolamine solution buffered at pH 8.1), adding a known quantity of magnesium sulphate solution, and then titrating the excess magnesium with ethylene-diamino-tetra-acetate (EDTA). The difference between added and titrated Mg is equivalent to the CEC of the sample. A duplicate sample plus an ‘‘in-house’’ QC sample was run with every batch of samples (14 maximum).

Soil pH was determined using a solid body pH electrode in a slurry composed of a soil sub-sample re-suspended in a 0.01 M CaCl2 solution. The method has UKAS and MCERTS accreditation and is validated for all soils with a pH between 3 and 10.

Total organic carbon (TOC) was measured on a ca. 1 g sediment sub-sample, which was oven dried at 100–105 8C for >1.5 h and re-weighed to obtain a ‘‘dry-weight’’. The sample was then treated with excess HCl acid (50%, v/v) to remove the inorganic carbon content, oven dried, and then analysed for carbon using an ‘Elementar Vario Max’ C/N analyser. Total carbon (TC) was analysed in the same way (without the acidification step) and then total inorganic carbon (TIC) was calculated as the difference between the two analyses. All data is reported as percentage of carbon.

Samples for loss on ignition (LOI) analysis were first oven dried overnight at 105 8C, and then LOI was calculated as the weight difference before and after heating for 1 h at 1050 8C. Quality control (QC) was monitored by the regular analysis of three materials covering the range of LOI values found in most geological materials.

Water content measurements were made by accurately weighing ca. 30 g of sediment in an aluminium container, and subsequently calculating the weight loss after heating at 80 8C for 24 h. Values are reported as (g water/g wet sediments) □ 100.

Major and minor oxides were measured on 40 mm beads prepared by fusing 0.9000 g sample and 9.000 g flux (66/34 Li2B4O7 and LiBO2) at 1200 8C. Analyses were conducted using a Philips MagiX-PRO WD-XRFS, equipped with a 60 kV generator and 4 kW rhodium (Super Sharp) end-window X-ray tube and controlled via a PC running the PANalytical SuperQ XRF application package. All spectral backgrounds and peaks were corrected for instrument drift using two external ratio monitors and inter-element effects were corrected using theoretical alpha coefficients. Quality control was monitored by the analysis of two bulk rock materials chosen for their variety of type and analyte values.

Trace elements were measured on pressed powder pellets formed by grinding 12.00 g of sample and 3.00 g of binder in an agate planetary ball mill for 30 min and then pressing at 25 tonnes load. Analyses were conducted using an Axios Advanced Spectrometer WD-XRFS, equipped with a 60 kV generator and 4 kW rhodium (Super Sharp Max) end-window X-ray tube and controlled via a PC running the PANalytical SuperQ XRF Pro-Trace application package. This package was used to correct for matrix effects (using mass attenuation coefficients) and interference from background, tube spectral lines, and spectral line overlap. A set of synthetic standards (Pro-Trace) was used to calibrate the instruments and to determine background and spectral interference correction factors. The calibrations were validated by analysis of a wide range of reference materials, and quality control was maintained by regular analysis of two glass monitor samples containing 47 elements at nominally 30 and 300 ppm.

3.4. Botany

Botanical surveys were conducted along the entire length of the transect, visually defining the percentage cover of identified plant groups at 0.5 m intervals using a 0.5 m □ 0.5 m quadrat. Field flora books were used to identify plants (Blamey and GreyWilson,2004;Daviesand Gibbons,1993)anddigitalphotographs were taken of each quadrat during both campaigns for a complete visual record. Note that shortly before the June 2006 campaign the field had been harvested for animal feed, thus making botanical observations more difficult.

3.5. Microbiology

Epifluoresence microscopy was performed by adding □1–2 gof soil to pre-weighed containers having 10 ml of fixative solution (0.5% gluteraldehyde in cacodylate buffer) and storing at 4 8C. Samples were then vortex mixed for a few seconds, allowed to settle, and the supernatant used for analysis. In the laboratory, 5 ml of the supernatant was vacuum filtered onto a 0.2 mm polycarbonate filter (Millipore) and a fluorochrome dye, acridine orange, was added to stain the nucleic acids. After 2 min staining the filter was mounted onto a glass slide and the total number of bacterial cells were counted in twenty fields of view using a Zeiss microscope fitted with a short wavelength mercury vapour light source. Results were then averaged for the 20 fields of view and are reported as number of bacteria per gram of sample.

Adenosine triphosphate (ATP) microbial biomass analyses were conducted on sample supernatant using a DeltaTox analyser and extractants supplied by Strategic Diagnostics, Inc. (SDI Europe Ltd.). Analyses followed the Deltatox protocol; in September 2005 analyses were conducted up to 12 h after collection in the hotel room, while June 2006 samples were processed immediately in a mobile laboratory. In summary, sub-samples of □1–2 g of soil were placed in sterile bijou containers, weighed, vortex mixed for a few seconds with 2 ml of deionised water, and then allowed to settle. A 100 ml sub-sample of the supernatant was then transferred to a glass cuvette and 100 ml of both ATP extractant and reagent were added at specified time intervals. The cuvette was then placed in the Deltatox analyser. ATP in the sample reacts with the reagents and the light output of this reaction is measured. The amount of ATP in the sample is directly proportional to the total biomass present of the sample. The error in the ATP analyses is estimated to be approximately □5%.

Quantitative polymerase chain reaction analyses (qPCR) first involved the extraction of high molecular weight DNA from soil samples, stored at □20 8C, via cell lysis and DNA purification. Cell lysis was achieved by adding a 10% lauryl-sulphate solution and zirconium-silica beads to the soil sub-sample and shaking for 45 s; subsequent DNA purification was performed using NH4-acetate and isopropanol precipitations (Henckel et al., 1999). Eubacteria and Archaea nucleic acids were quantified by real-time qPCR (Lu¨ ders et al., 2004) using an ABI Prism 7000 Sequence Detection System (Applied Biosystems, Germany) and primer sets Ba519f/Ba907r and Ar109f/Ar912r, respectively. The gene copy numbers (n = 12, standard error (S.E.)) were converted into cell numbers using a conversion factor of 3.6 and 1 for Eubacteria and Archaea, respectively (Klappenbach et al., 2001).

Three soil samples along the profile were also measured for (i) methane production rates (MPR), (ii) methane oxidation rates (MOR), and (iii) sulphate reduction rates (SRR). Preparation for all three incubation experiments first involved the conversion of soil samples into slurries by the addition of autoclaved and deoxygenated tap water in a ratio of 1:1 (w/w). All manipulations were performed in 3–5 replicates under a N2/CO2 (90/10, v/v) atmosphere in an anoxic glove chamber (Mecaplex), while the subsequent incubations were performed at 20 8C in the dark (Kru¨ ger et al., 2001). Microbial activities were calculated by linear regression of the product increase or decrease with incubation time, and expressed in mmol sulphide or methane produced or oxidised per gram dry weight of soil (gdw soil□1) per day of incubation time (d□1) (n = 3–5, □standard error (S.E.)). Specific details of these three experiments follow.

Three replicates of 10 ml slurry from each soil sample were repeatedly flushed with N2 (to remove residual O2) and incubated in Hungate tubes (16 ml) to determine the initial potential MPR (Kru¨ ger et al., 2001). Another three replicates of each sample were used to determine the fraction of methane produced from H2/CO2 (fH2), using a final concentration of 0.5% methyl fluoride (CH3F 99%, ABCR Karlsruhe, Germany) as a specific inhibitor of acetate-dependent methanogenesis (Kru¨ ger et al., 2001). Headspace gas samples were taken daily after heavy shaking of the tubes by hand, and analyzed for methane and methyl fluoride (to ensure a constant inhibitor concentration) on a gas chromatograph equipped with a flame ionization detector. The fH2 was calculated by comparing the MPR after addition of methyl fluoride to those in the control tubes.

Potential MOR were measured in the same soil samples as described for methane production. Triplicate 10 ml slurries were transferred into sterile serum bottles (50 ml), sealed with butyl rubber stoppers, and methane was added to a final concentration of 10% in the headspace. Methane depletion was monitored by sampling the headspace, with the first sample taken after 60 min, followed by sampling at daily intervals.

Incubations to determine the sulphate reduction rates (SRR) were set up as described above for MPR, but with the addition of sulphate from an anoxic stock solution to a final concentration of 10 mM. Sulphate reduction was monitored by measuring the evolving formation of copper sulphide (Cord-Ruwisch, 1985).

4. Results

4.1. Gas geochemistry

A summary of some of the soil gas results obtained from 20 cm depth during the September 2005 and June 2006 campaigns are presented in Fig. 2. The general trends of all species are reproducible in the two different seasons, although the higher sampling density in 2006 gives better spatial resolution. This is particularly true for methane, ethane and hydrogen sulphide in the vent centre, where limited sampling and a lost sample at 5 m in the 2005 data gives a false impression. More detailed, deeper sampling (80 cm) performed during the September 2005 campaign (not shown) and other research conducted on the same site (Annunziatellis et al., 2008) show the same general trends observed in the June 2006 results. Fig. 2 shows a direct negative correlation between CO2 and O2 +Ar (r 2 = 0.997; y = 20.31 □ 0.20x) and CO2 and N2 (r 2 = 0.998; y = 77.96 □ 0.76x), with the bulk of O2 + Ar and N2 decrease being caused by dilution with CO2 (see slopes of correlation lines). The centre of the vent is almost anoxic even at this shallow depth, beyond which CO2 concentrations decrease rapidly for the first couple of metres and then decrease slowly towards background values of <2% around 25–30 m. In contrast, anomalous values of the more reactive species, like methane, occur in a narrow interval in the centre of the vent, while insoluble and non-reactive helium has a distribution which is intermediate between these two extremes. CO2 flux is plotted both on a linear and a logarithmic scale in Fig. 2, showing a rapid change in rates at about 8 m on the linear scale and a more subtle change at about 25 m on the log scale.

4.2. Grain size, mineralogy, and soil chemistry

Particle size analyses confirm the field observations that the soils are all clay to heavy clays. 'Sedigraph' analyses of the <63 mm fractions indicate that all samples have a very similar particle size distributions, being dominated by the clay and silt fractions. There are no systematic variations in soil texture along the transect.

In terms of bulk mineralogical compositions the analysed samples are relatively similar, with the major constituents being quartz, K-feldspar, and pyroxene (augite), with minor amounts of hematite and albite, and trace amounts of cristobalite, mica, and pyrite. The clay assemblage is dominated by halloysite with typically less than 20% illite. The high backgrounds observed in the XRD results indicate that a significant proportion of amorphous, non-crystalline material is present in the soils, which is most likely volcanic glass derived from underlying sediments. It should be noted therefore that the reported mineral percentages are only relative to total inorganic crystalline minerals and do not include variations in non-crystalline volcanic material or organic components.

The results for various mineralogical, chemical and physical parameters measured in September of 2005 are plotted along the transect in Fig. 3. Over the first 15 m of the transect mineral phases like K-feldspar, quartz, and ''mica'', trace elements like As (and Cr), and parameters like LOI, CEC, and TOC all increase towards the vent centre on the left. In this same interval decreasing trends are seen in soil pH, in minerals like augite, albite, and cristobalite, oxides like CaO, MgO, Fe2O3 and Mn3O4, minor elements like Ba (and Rb, Sr), and trace elements like Co (and Ni, Cu, Zn, V). Various other trace elements do not show a regular trend.

Water content measurements for both field campaigns show a minimum just outside the central part of the vent (i.e. from 8 to 14 m), bounded by the highest values within the vent and by relatively constant intermediate values away from the vent (Fig. 3). Note the slightly higher background values during the wetter fall compared to the dryer summer.

4.3. Botany

The results of the botanical surveys conducted in September 2005 and June 2006 are given in Fig. 4, with plots shown for the percentage cover of bare earth, die-back (i.e. essentially dead

No vegetation grows in the centre of the vent (which is just bare earth), while what appears to be acid-tolerant grasses (Agrostis capillaris) begins from 6 to 7 m in both surveys. In the September survey the grasses then appear to dominate the transect from □9 m until □25 m, after which clover starts to become the dominant plant. In contrast, grasses dominate along most of the profile in June. The patches of die-back, which occurred in the 8–15 m section of the transect in September, appear to have shifted to the 12–18.5 m position in June. There are also patches of moss visible at 5.5–8.5 m in the June survey that were not apparent in the previous September survey.

4.4. Microbiology

Fig. 5a shows the microbial biomass results, obtained using ATP analysis, for both field campaigns; the trends of the two profiles are generally similar, although absolute values are different ($p = 0.027$). Although these differences in values may be due to seasonal effects, it should be noted that the 2006 data may be of higher quality due to immediate analysis in a mobile laboratory. In general the ATP concentrations within the vent centre (at 2 and 5 m) are very low, increase sharply over the interval from

8 to 15 m, and then decrease to relatively low values in the background area (except for the high value at 35 m in June 2006).

The total bacterial count results, obtained with epifluorescence microscopy, show a simpler trend (Fig. 5b) which is quite reproducible for the two different sampling seasons (for example, excluding the questionable point at 50 m in the 2006 data, r 2 =0.82 and p = 0.005). Here values are low within the vent, and then are higher and relatively constant from about 9–50 m. Interestingly the point of change at around 9 m appears to be the same for both sampling seasons, despite the significantly different environmental conditions.

The number of bacteria cells obtained using quantitative PCR (Fig. 5c) also appear to change near 9 m, although the limited sampling with this technique does not allow exact trends to be defined. It should be pointed out that the absolute values of the microscopic cell counts obtained using epifluorescence and qPCR are quite different. This may be explained by the potentially very-strong adhesion of bacteria to soil particles or organic matter (Bakken and Lindahl, 1995; Lunau et al., 2005), or by the qPCR amplification of free DNA still remaining in the soil after lyses of the cells (which thus escapes microscopy). The qPCR data for archaea numbers, in contrast to those for bacteria, remain low at 9 m and are higher only at the 50 m sample (Fig. 5c).

Methane production, methane oxidation, and sulphate oxidation rates were measured on three samples collected in June of 2005 at 3 m (vent core), 9 m (transition zone) and 50 m (background) along the transect. Methane production rates (MPR) at the background site were 2.34 □ 0.35 nmol CH4 produced gdw soil□1d□1, three times higher than in the vent core with high CO2 and H2S(0.79 □ 0.13) and eight times higher than in the transition zone with high CO2 but no H2S (0.29 □ 0.03). The addition of methyl fluoride (CH3F) as a selective inhibitor for acetate-dependent methanogenesis (Kru¨ ger et al., 2002) led to a substantial reduction of MPR at the backgroundsite(i.e. from2.34 □ 0.35to0.81 □ 0.18 nmolCH4 produced gdw soil□1d□1) but had no effect at the CO2-rich sites. The activity of aerobic methane oxidising bacteria (MOB) also showed a negative response to high CO2 concentrations, with rates at the background site (0.95 □ 0.06 mmol CH4 oxidised gdw soil□1d□1) being almost double those measured in the vent core (0.48 □ 0.09) and transition zone (0.53 □ 0.05) samples.

5. Discussion

A comparison of some representative biological and geochemical data presented in Figs. 2–5 is given in Fig. 6 (wetter growing season of September, 2005) and Fig. 7 (dry harvest period of June, 2006) for the interval 0–35 m; background values from 35 to 50 m have been removed from these two figures to improve legibility. Not all the same measurements were conducted during the two field seasons and thus these plots do not always show the same types of data. In addition there is variable sample spacing for the different techniques, and thus correlations are sometimes approximate.

For discussion purposes the transect has been divided into three zones. Moving from right to left in the figures, that is towards ever increasing effects induced by the gas vent, the zones are: 1, background; 2, transition; and 3, vent core. These intervals are shown on the top of Figs. 6 and 7 for reference.

5.1. Zone 1—background

The background interval occurs from 50 to 30 m, based on the constant soil gas and gas flux values (Fig. 2) that are in the range of values produced by near-surface biogenic processes (e.g. [CO2] <2% and fCO2 < 10 g m□2d□1). Botanical (Fig. 4), ATP and epifluorescence (Fig. 5), and water content (Fig. 3) results are also relatively constant across zone 1, whereas it is not possible to define trends in many of the solid chemistry data (Fig. 3) because of low sample density.

5.2. Zone 2—transition

Increasing soil gas CO2 concentrations, from 30 to 7 m along the profile, define a 23 m wide transition interval between

5.2.1. Zone 2a

The first minor changes in the system caused by the presence of the gas vent are observed in zone 2a (from 30 to 14 m), however they are relatively small and primarily restricted to the addition of CO2 rather than the secondary effects caused by the CO2. For example, soil gas CO2 increases from 2 to 11%, O2 decreases from 20 to 18%, CO2 flux increases from 3 to 35 g m□2d□1, and pH decreases from 5.2 to 4.5. In contrast, many soil chemistry and microbial parameters that could potentially be altered by CO2 addition are constant across zone 2a (e.g. water content, bacteria cell counts, ATP biomass, Fe3O2, albite and K-feldspar) or do not have a clearly definable trend (e.g. CaO, MgO). There does appear to be some subtle changes in vegetation, however the different behaviour between the two sampling campaigns makes any trends difficult to define. For example, in the September 2005 data there appears to be a general exchange of dominance between grass and clover, particularly after 20 m (Fig. 6), while there is no such trend in the June 2006 data (Fig. 7). While this difference could be related to seasonal changes, such as the hot and dry conditions during June 2006, it should be noted that shortly before the June field campaign the field had been harvested for animal feed, thus making botanical observations more difficult. The fact that the field is grazed and harvested (although not planted and cultivated) means that botanical trends may be slightly affected by limited human intervention.

5.2.2. Zone 2b

The first significant effects of the gas vent are observed in zone 2b (from 14 to 9 m), not only in CO2 distribution (which increases at a rate of 500 ppm cm□1) but also in many other biological and geochemical parameters. In particular, this interval appears to be important in terms of physical transport of gases and geochemical reactions.

For example, zone 2b corresponds with a water content minimum, which is best observed in the wetter season (Fig. 6) but which also occurs in the dry season data (Fig. 7). This interval of dryer soil will have a higher effective gas porosity and permeability, which in turn will greatly aid in transporting CO2 and other deep gases away from the vent core and atmospheric O2 towards it. The cause of this minimum is not clear, however possible mechanisms include: (i) the downward, convective flow of dry atmospheric air induced by the high upward flux rates in the vent core; (ii) the consumption of water via the precipitation of hydrous mineral phases, such as the oxidation of H2S to gypsum (CaSO4□2H2O); or (iii) enhanced soil moisture removal by plants near the vent. Detailed field experiments would be needed to illustrate the first option, whereas the second is considered unlikely because of the lack of increased sulphate minerals in this interval. In regards to option three, various studies have shown that increased atmospheric CO2 concentrations (as would occur in the canopy of grass near the vent centre) have an effect on plant water uptake. Many studies have shown that increased CO2 values result in decreased stomatal conductance and thus an increase in soil moisture content (e.g. Robredo et al., 2007), however others have suggested that such behaviour is species dependant and that soil moisture can actually decrease due to increased plant growth and root biomass (Moore and Field, 2006). These latter authors also illustrate that under elevated atmospheric CO2 concentrations some species increase the efficiency of their deep roots, extracting a larger percentage of water earlier from deeper intervals.

For both sampling campaigns, maximum ATP biomass values occur within zone 2b and appear to correspond with the water content minimum, whereas bacterial cell counts remain essentially constant across this interval. This curious relationship may be related to the discussion above on the influence of atmospheric CO2 concentrations, as increased root biomass can increase growth, turnover, and respiration in soil systems (Moore and Field, 2006) and increase root/microbe symbiotic biomass (Rillig et al., 2000). Soil pH values drop quickly across zone 2b (from 4.5 to 3.8), which results in a clear influence on the chemical composition of the soil. Most oxide concentrations begin to decrease at the outer edge of zone 2b (i.e. at 14 m) while parameters such as cation exchange capacity, loss on ignition, and total organic carbon begin to increase (Figs. 3 and 6). As discussed in more detail below for zone 3, these values are changing in response to decreasing pH values and O2 concentrations across zones 2b, 2c and 3, which increases weathering and mineral dissolution and decreases organic matter oxidation.

The main botanical change observed across zone 2b is the disappearance of clover and ‘‘other’’ plant groups (indicating decreased diversity) at about 13 m during both surveys (Figs. 6 and 7). This corresponds to 5% CO2 at 10 cm depth, 20% CO2 and 17% O2 at 20 cm depth, and a pH of <4.5, low water content and high ATP biomass in the 0–20 cm depth interval. These results, combined with the observation that grasses exist throughout this interval, suggest that dicotyledonous plant species (e.g. clover) are less tolerant of elevated CO2 concentrations than monocotyledonous plant species (e.g. grasses). This could be related to the fact that clover is a legume with root nodules containing essential nitrogen-fixing microorganisms (e.g. Vessey et al., 2005), and it may be that elevated soil CO2 affects the activity of these organisms. It must be pointed out, however, that other factors such as photosynthetic pathway, plant age, and nitrogen concentration may produce similar results, and thus more research is needed to understand the actual mechanism of clover disappearance.

In addition to the disappearance of clover there is an enhanced amount of ‘‘die-back’’ in zone 2b in the September 2005 data (Fig. 6), indicating that the remaining plant types (principally grass) are living under stressed conditions, possibly due to the combined effects of elevated CO2 concentrations and low water content. This relationship is not seen in the June 2005 data (Fig. 7), however it must be remembered that the vegetation is generally stressed by the high temperatures and low rainfall during the summer period, and thus it may be more difficult to highlight gas vent induced stress during this season compared to the wetter and cooler fall.

5.2.3. Zone 2c

The greatest lateral changes in soil gas concentration (at 20 cm depth) are observed in zone 2c (from 9 to 7 m), where CO2 increases at 5600 ppm cm^{-1} in June and 3400 ppm cm^{-1} in September, and O2 + Ar decreases at 1300 and 800 ppm cm^{-1} during the same periods. The maximum CO2 vertical gradient, measured across the 10–20 cm depth interval, is about 2% cm^{-1} around 7–8 m. CO2 flux rates also change significantly across zone 2c, although the limited number of samples taken in this interval make it difficult to define trends (Fig. 7). These rapidly changing conditions related to the upward migration of the deep gases have a significant effect on numerous parameters.

One example is the complete absence of H2 (not shown), and CH4,C2H6, and H2S(Figs. 2 and 7) in zone 2c compared to the very high concentrations of these gases in the adjoining zone 3. Zone 2c must therefore be an important interval for the oxidation of these redox reactive species. In particular, the plot in Fig. 7 shows how the reactive gas species appear at the contact between zones 2c and 3 when CO2 flux rates begin to increase rapidly and conditions become essentially anoxic.

Water content values in zone 2c are only slightly higher (Fig. 6) or equivalent (Fig. 7) to the low values observed in zone 2b, and thus, as discussed above, the presumed higher effective gas permeability likely plays an important role in the outward migration of CO2 and the inward diffusion of O2 (which is, in turn, likely linked to the oxidation of the redox-reactive species in this zone discussed above). Insufficient geochemical analyses in this interval do not allow for any trends to be defined for parameters such as mineralogy, bulk chemistry, and pH.

Soil biological changes that occur across zone 2c include the marked decrease in ATP biomass and bacterial cell counts, likely also related to the increasingly anoxic conditions. Interestingly the decrease in bacterial cell count data occurs across zone 2c for both seasons (Fig. 5b), implying that the bacterial system is equilibrated with the vent structure and little influenced by changing environmental conditions. Archaea values are quite low in this interval relative to the background site (Fig. 5c) and, unlike the bacteria numbers, are similar to those observed in the vent core; this suggests that archaea are more sensitive to the higher CO2 concentrations, which is surprising considering that these microbes are often found in extreme environments. The single sample analysed in this interval for methane production rates (MPR) was particularly low, being only 12% that observed in the background sample and 37% of that in the vent core; this low methane production rate may be linked to the very low water content occurring in this interval.

Finally the vegetation within zone 2c becomes increasingly stressed, occurring commonly as isolated tuffs of grass surrounded by die-back closer to the vent core and disappearing altogether at the contact between zones 2c and 3 (Figs. 6 and 7). During both field campaigns an acid-tolerant grass (A. capillaris) was found in this interval (as well as in zone 2b). This grass is able to survive in zone 2c in surprisingly high CO2 concentrations (15–40% at 10 cm depth), similar to that observed for some grasses at the Stavesinci site in Slovenia (Macek et al., 2005; Pfanz et al., 2007; Vodnik et al., 2006). It is quite possible that adaptation has allowed it to survive in such a high CO2, low pH environment, as proposed for other studied sites (Pfanz et al., 2007; Selvi, 1997). For example, Pfanz et al. (2007) show how timothy grass (Phleum pratense L.) living in high soil-gas CO2 concentrations appears to have adjusted its respiration and photosynthetic carbon assimilation rates compared to the same species living under near-by background conditions.

5.3. Zone 3—vent core

As stated previously the vent core (zone 3) is about 6 m wide and is recognised by a total lack of vegetation, likely caused by the combined effects of CO2 flux rates near 2000 g m□2d□1, soil gas CO2 near 100% (even at 10 cm depth), O2 +Ar at <1% (remember that atmospheric [Ar] □ 0.9%), the presence of elevated concentrations of reduced gas species like CH4 and H2S, and soil pH values between 3.5 and 4. Although the main mechanism preventing plant growth is not clear, these conditions will certainly affect nutrient availability or uptake (Pfanz et al., 2007), root functioning (Macek et al., 2005; Vodnik et al., 2006), and respiration (Farrar et al., 1995), and the above ground processes of photosynthesis (Pfanz et al., 2007), transpiration (Tognetti et al., 2000) and respiration.

The combined effect of acidic and essentially anoxic conditions have resulted in a series of mineral and bulk chemistry transformations. For example, there appears to be a sharp decrease in albite content, and corresponding increase in K-feldspar, across the boundary between zones 3 and 2c. Modelling of the Sleipner caprock shows that the CO2mediated dissolution of albite and precipitation of K-feldspar is thermodynamically possible under those in situ conditions (Gaus et al., 2005). The occurrence of these reaction products here imply that this is a valid pathway and that the gas vent has existed for sufficient time to form these minerals despite the potentially slow kinetics at ground-surface temperatures. In addition the decrease in various oxides (like MgO, CaO, Fe2O3 and Mn3O4) observed across zones 2b and 2c continues into zone 3, due again to the combined anoxic and acidic conditions.

Although a number of trace metals were found to be depleted in the vent core, likely due to the dissolution of primary phases, differences are not large and it appears that large-scale leaching from the A horizon has been prevented via precipitation within secondary mineral phases or adsorption related to the increased CEC and TOC. More detailed work involving sequential extractions and detailed petrography would be needed, however, to better understand the exact processes and pathways.

The observed increase in CEC and TOC, as well as LOI, within zone 3 is likely due to the reducing conditions, which allow for the preservation of organic matter. This interpretation is supported by the discovery of unaltered plant rootsatadepth ofabout60 cmat5 m, despite the totallack of plant life above it. The higher TOC values observed in the vent core are in contrast to that observed by Stephens and Hering (2002) in high CO2 soils at Mammoth Mountain, possibly due to the greater sample depth in that study (B instead of A horizon), but agree with the low cycle of organic matter decomposition hypothesised by Selvi (1997) based on microbial data from various Italian gas springs. The TOC results also agree with biogeochemical modelling of CO2 intrusion into the vadose zone which shows how the displacement of O2 by CO2 transfers organic matter oxidation to the much slower NO3 electron acceptor pathway (Altevogt and Jaffe, 2005). The rise in CEC may also be influenced by the more aggressive environment within zone 3, as acid-induced alteration products can increase grain surface areas (Stephens and Hering, 2002).

Water content values are highest in zone 3 compared to the rest of the profile for both seasons, probably due to the flux of water-saturated gas from the water table and the lack of evapo-transpiration in this non-vegetated interval. Stephens and Hering (2002) also attributed higher water content values observed in high-CO2, tree-kill areas to the lack of evapo-transpiration, however at that site the effect was only observed at the end of the dry season and not after the snow melt period. In any case, the consistently high water content in this interval, combined with the low pH values, creates an environment that favours the geochemical reactions described above.

The decreasing trends in ATP biomass and bacterial cell counts observed in zone 2c continue in zone 3, with the bacterial numbers at 2 m representing the lowest values along the entire transect. Despite this low biological activity, incubation experiments have shown that some microbes are able to take advantage of the in situ conditions. For example, the strictly anaerobic sulphate-reducing bacteria have their highest activities in the centre of the vent, stimulated by the absence of oxygen and perhaps the presence of nutrients like organic carbon and hydrogen. A second anaerobic group, the methanogenic archaea, also show higher activities in the centre of the vent compared to the transition zone site. Interestingly, H2-dependent methanogenesis is essentially absent in the vent core; because this major methanogenic pathway accounted for almost half of total methane production at the control site, its absence here indicates that it is completely inhibited in high CO2 environments. Aerobic methane oxidation is also negatively affected by the high CO2 concentrations and oxygen limitation.

Finally the presence of reduced gas species like H2S, H2, CH4, and C2H6 is limited to zone 3, where it appears that a sufficient CO2 flux is needed to prevent oxidation. The reason for this is likely linked to the maintenance of sufficiently low O2 concentrations and short residence times in the soil horizon. Laterally, as described above, these gases are rapidly oxidised and returned to background soil gas values within zone 2c.

5.4. Comparison with hypothetical leakage rates

To put the impact of this gas vent in context we can compare its total CO2 output with a hypothetical leak from a geological storage site. Various computer models have been used in the literature to calculate the amount of CO2 leakage, from geological CO2 storage reservoirs to the atmosphere, that would be acceptable from the point of view of mitigating global warming. These studies typically report that values less than 0.1% (Teng and Tondeur, 2007; White et al., 2003) or 0.01% (Hepple and Benson, 2002) per year of the total stored CO2 are needed to ensure the stabilisation of atmospheric CO2 concentrations at set limits. Using the lower leakage rate of 0.01% and applying it to a hypothetical geological reservoir with 10 Mt of stored anthropogenic CO2 would result in a daily emission rate of about 2700 kg d□1.This value is approximately 10 times greater than the total output of this gas vent (220 kg d□1).

It must be remembered, however, that the spatial release of a given mass of CO2 at surface will be site specific, depending strongly on how the gas migrates at depth (e.g. number and size of pathways) and in the shallow subsurface (e.g. depth to water table) (Annunziatellis et al., 2008). The number of release points thus becomes critical in understanding the potential impact on the ecosystem.

For example, if all of the hypothetical release of 2700 kg d□1 occurred from this gas vent, instead of the measured 220 kg d□1, it is possible that the size and ecosystem impact would be only a limited amount greater than that presently observed (i.e. not 10 times greater). This is because increased flow might be preferentially channelled through the non-vegetated core as it is now, and thus the surrounding impact would again be regulated by lateral advection and diffusion of CO2. It is expected that the transition zone would be forced outwards due to the higher horizontal pressure gradient, but that its eventual distance would be regulated by the larger cylindrical volume occupied by the transition zone (i.e. pressure dissipation) and downward migration of atmospheric air. Although the impact on the near-surface ecosystem may be only slightly larger in this scenario, clearly the risk for accumulation would be higher.
If, instead, the hypothetical release occurred from 10 separate points there would be the potential for the formation of 10 gas vents similar to the one examined in this research. This would result in a larger

impact on the near-surface ecosystem but a lower risk for accumulation. A continued increase in the number of release points would decrease the flux from each vent, which in turn would decrease the effect on the shallow ecosystem (to the point where it would no longer be noticeable) and decrease the risk of accumulating dangerous quantities of CO2 near the ground surface.

It must be remembered, however, that these calculations are made using leakage rates defined on the basis of global warming mitigation goals and not on site specific geological conditions, which would be expected to be much lower in a well-chosen geological CO2 storage site. For example, a leakage rate of 0.001% would result in a total mass transfer rate similar to that observed for this gas vent. Again the number and distribution of gas release points at the surface would then control any potential impact on the near-surface ecosystem.

6. Conclusions

Detailed geochemical and biological sampling across a natural CO2 gas vent has defined the impact of this leak (220 kg CO2 d□1) on the near-surface ecosystem of a Mediterranean pasture. Although this site within the Latera caldera (central Italy) is not considered an analogue of an industrial geological CO2 storage site (because of extensive faulting and the ‘‘limitless’’ supply of thermo-metamorphically produced CO2), it can be used as a test site to better understand the potential impact of CO2 in the near-surface environment should leakage occur.

Measurements along a transect crossing the gas vent have shown that soil gas CO2 concentrations and CO2 flux rates above background values occur out to a distance of 25 m from the centre of the vent. In contrast, however, the first measurable changes to the near-surface ecosystem (e.g. decreasing pH and oxides, increasing ATP biomass and organic matter content, low water content, and altered vegetation types) occur at about 9 m from the vent centre, while highly significant changes (e.g. anoxia, soil pH < 3.5, changes in mineralogy, reduced microbial activity, and lack of vegetation) begin at about 3 m. Thus, under the conditions occurring at this site the measurable impact of a 220 kg d□1 CO2 release on the near-surface environment covers a total area of about 250 m2 while the highly significant impact is restricted to a vent core of about 28 m2.

This study has shown the intricate and complex interaction amongst the physical aspects of gas movement (both CO2 away and O2 towards the vent core), the chemical reactions caused by leak-induced low pH and Eh values, the distribution of soil water content, and the types (and health) of microbes and plants living in an environment that changes radically over the space of a few metres. For example, a certain grass type appears to have been able to adapt to the high soil gas and atmospheric CO2 concentrations and low pH and water content conditions near the vent core, while clover appears to be much less tolerant of these conditions. Another interesting observation is the fact that there does not appear to be large-scale leaching of trace metals from the vent core despite the very low pH values, likely due to immobilization onto increased cation exchange capacity and total organic matter caused by the low pH and the anoxic conditions.

Finally the comparison of this leak with a hypothetical leak of 0.01% per year (based on global warming criteria rather than measured geological parameters) from a large 10 Mt geological CO2 storage site has shown that the hypothetical leak would result in a mass transfer of about 2700 kg d□1 compared to the 220 kg d□1 coming from this Latera gas vent. Considering, however, that a well-chosen CO2 storage site will have few or no significant leakage pathways, it is expected that actual leakage from a geological CO2 storage site (if it occurs at all) would be significantly lower than the non site-specific rate of 0.01%. In any case the impact on the ecosystem of any leak will depend significantly on its migration pathways at depth and eventual spatial distribution on the surface, in that the more release points there are the more the flow will be divided and thus the lower the impact will be.

Acknowledgements

The present work was conducted within the framework of CO2GeoNet, a European Community funded ‘‘Network of Excellence’’ dedicated to the study of all aspects of geological CO2 storage. Funding from the EC is gratefully acknowledged, as is funding from each of the author’s institutions. The authors would also like to highlight the important contribution of numerous colleagues to this study, both in the field and the laboratory: Cathy Scheib, Richard Shaw, Julian Trick, Ian Webster, Doris Wagner, Barbara Vickers, Mark Ingham, Heather Harrison, and Simon Kemp (BGS), Monia Coltella and Anna Baccani (URS), Cornelia Haveland (BGR) and Catherine Joulian (BRGM). Finally we would like to thank the land owner of the study site, Mr. Iacarelli, for access to the site, and two anonymous reviewers for their very useful comments. PC, JMP and JMW publish with the permission of the Executive Director, BGS (NERC).

References

Altevogt, A.S., Jaffe, P.R., 2005. Modelling the effects of gas phase CO2 intrustion on the biogeochemistry of variably saturated soils. Water Resour. Res. 41 (W09426), doi:10.1029/ 2004WR003819.
Annunziatellis, A., Beaubien, S.E., Bigi, S., Ciotoli, G., Coltella, M., Lombardi, S., 2008. Gas migration along fault systems in the Latera natural analogue (central Italy): implications for CO2 geological storage. Int. J. Greenhouse Gas Control 2 (3), 353–372.
Bachu, S., Gunter, W.D., 2004. Acid-gas injection in the Alberta basin, Canada: a CO2 storage experience. In: Baines, S.J., Worden, R.H. (Eds.), Geological Storage of Carbon Dioxide, vol. 233. Geological Society of London, London, Special Publications, pp. 225–234.
Bakken, L.R., Lindahl, V., 1995. Recovery of bacterial cells from soil. In: Trevors, J.T., van Elsas, J.D. (Eds.), Nucleic Acids in the Environment: Methods and Applications. Springer, pp. 9–27.
Bateson, L., Vellico, M., Beaubien, S.E., Pearce, J.M., Ciotoli, G., Annunziatellis, A., Coren, F., Lombardi, S., Marsh, S., 2008. Preliminary results of the application of remote sensing techniques to detecting and monitoring leaks from CO2 storage sites. Int. J. Greenhouse Gas Control 2 (3), 388–400.
Biondi, F., Fessenden, J.E., 1999. Response of lodgepole pine growth to CO2 degassing at Mammoth Mountain, California. Ecology 80 (7), 2420–2426.
Blamey, M., Grey-Wilson, C., 2004. Wild Flowers of the Mediterranean. A and C Black Publishers Ltd., London, UK.
Chadwick, A., Arts, R., Eiken, O., Williamson, P., Williams, G., 2006. Geophysical monitoring of the CO2 plume at Sleipner, North Sea. In: Lombardi, S., Altunina, L.K., Beaubien, S.E. (Eds.), Advances in the Geological Storage of Carbon Dioxide. NATO Science Series. Vol. IV. Earth and Environmental Sciences, vol. 65. Springer, Dordrecht, The Netherlands, pp. 303–314.
Chiodini, G., Cioni, R., Guidi, M., Marini, L., Raco, B., 1998. Soil CO2 flux measurements in volcanic and geothermal areas. Appl. Geochem. 13, 543–552.
Ciotoli, G., Guerra, M., Lombardi, S., Vittori, E., 1998. Soil gas survey for tracing seismogenic faults: a case study in the Fucino basin, central Italy. J. Geophys. Res. 103 (B10), 23781–23794.
Ciotoli, G., Etiope, G., Guerra, M., Lombardi, S., 1999. The detection of concealed faults in the Ofanto Basin using the correlation between soil-gas fracture surveys. Tectonophysics 301, 321–332.
Cook, A.C., Tissue, D.T., Roberts, S.W., Oechel, W.C., 1998. Effects of long-term elevated [CO2] from natural CO2 springs on Nardus stricta: photosynthesis, biochemistry, growth and phenology. Plant Cell Env. 21 (4), 417–425, doi:10.1046/ j.1365-3040.1998.00285.x.
Cord-Ruwisch, R., 1985. A quick method for the determination of dissolved and precipitated sulfides in cultures of sulfate-reducing bacteria. J. Microbiol. Methods 4, 33–36.
Davies, P., Gibbons, B., 1993. Field Guide to Wild Flowers of Southern Europe. Crowood Press Ltd., Wiltshire, UK.
Duchi, V., Minissale, A., Paolieri, M., Prati, F., Valori, A., 1992. Chemical relationship between discharging fluids in the Siena-Radiocfani Graben and the deep fluids produced by the geothermal fields of Mt. Amiata, Torre Alfina and Latera. Geothermics 21 (3), 401–413.
Farrar, C.D., Sorey, M.L., Evans, W.C., Howle, J.F., Kerr, B.D., Kennedy, B.M., King, C.Y., Southon, J.R., 1995. Forest-killing diffuse CO2 emission at Mammoth Mountain as a sign of magmatic unrest. Nature 376, 675–678.

Gaus, I., Azaroual, M., Czernichowski-Lauriol, I., 2005. Reactive transport modelling of the impact of CO2 injection on the clayey cap rock at Sleipner (North Sea). Chem. Geol. 217, 319–337.
Gumrah, F., Izgec, O., Gokcesu, U., Bagci, S., 2005. Modeling of underground gas storage in a depleted gas field. Energy Sources 27 (10), 913–920.
Henckel, T., Friedrich, M., Conrad, R., 1999. Molecular analyses of the methane-oxidizing microbial community in rice field soil by targeting the genes of the 16S rRNA, particulate methane monooxygenase, and methanol dehydrogenase. Appl. Env. Microbiol. 65, 1980–1990.
Hepple, R.P., Benson, S.M., 2002. Implications of Surface Seepage on the Effectiveness of Geologic Storage of Carbon Dioxide as a Climate Change Mitigation Strategy. GHGT-6, Kyoto, Japan.
Holloway, S., 1996. An overview of the Joule II project: ‘‘the underground disposal of carbon dioxide’’. Energy Convers. Manage. 37 (6–8), 1149–1154.
IPCC, 2007. Solomon, S., et al. (Eds.), Climate Change 2007: The Physical Science Basis. Contribution of Working Group I to the Fourth Assessment Report of the Intergovernmental Panel on Climate Change. Cambridge University Press, Cambridge, United Kingdom and New York, NY, USA, p. 996.
Jossi, M., Fromin, N., Tarnawski, S., Kohler, F., Gillet, F., Aragno, M., Hamelin, J., 2006. How elevated pCO2 modifies total and metabolically active bacterial communities in the rhizosphere of two perennial grasses grown under field conditions. FEMS Microbiol. Ecol. 55, 339–350.
Klappenbach, J.L., Saxman, P.R., Cole, J.R., Schmidt, T.M., 2001. rrndb: the ribosomal RNA operon copy number database. Nucleic Acids Res. 29, 181–184.
Kool, D.M., Chung, H., Tate, K.R., Ross, D.J., Newton, P.C.D., Six, J., 2007. Hierarchical saturation of soil carbon pools near a natural CO2 spring. Global Change Biol. 13, 1282–1293.
Kru¨ ger, M., Frenzel, P., Conrad, R., 2001. Microbial processes influencing methane emission from rice fields. Global Change Biol. 7, 49–61.
Kru¨ ger, M., Eller, G., Conrad, R., Frenzel, P., 2002. Seasonal variations in CH4 oxidation and pathways of CH4 production in rice fields determined by stable carbon isotopes and specific inhibitors. Global Change Biol. 8, 265–280.
Lewicki, J.L., Bergfeld, D., Cardellini, C., Chiodini, G., Granieri, D., Varley, N., Werner, C., 2005. Comparative soil CO2 flux measurements and geostatistical estimation methods on Masaya volcano, Nicaragua. Bull. Volcanol. 68, 76–90, doi:10.1007/s00445-055-0423-9.
Lombardi, S., Annunziatellis, A., Ciotoli, G., Beaubien, S.E., 2006. Near surface gas geochemistry techniques to assess and monitor CO2 geological sequestration sites. In: Lombardi, S., Altunina, L.K., Beaubien, S.E. (Eds.), Advances in the Geological Storage of Carbon Dioxide. NATO Science Series. Vol. IV. Earth and Environmental Sciences, vol. 65. Springer, pp. 141–156.
Lu¨ ders, T., Manefield, M., Friedrich, M.W., 2004. Enhanced sensitivity of DNA-and rRNA-based stable isotope probing by fractionation and quantitative analysis of isopycnic centrifugation gradients. Env. Microbiol. 6, 73–78.
Lunau, M., Lmke, A., Walther, K., Martens-Habena, W., Simon, M., 2005. An improved method for counting bacteria from sediments and turbid environments by epifluorescence microscopy. Env. Microbiol. 7, 961–968.
Macek, I., Pfanz, H., Francetic, V., Batic, F., Vodnik, D., 2005. Root respiration response to high CO2 concentrations in plants from natural CO2 springs. Env. Exp. Bot. 54, 90–99.
Moore, L.A., Field, C.B., 2006. The effects of elevated atmospheric CO2 on the amount and depth distribution of plant water uptake in a California annual grassland. Global Change Biol. 12, 578–587.
Pearce, J.M. (Ed.), 2004. Natural analogues for the geological storage of CO2. Final Report of the Nascent Project. British Geological Survey Technical Report, 122 pp.
Pettinelli, E., Passaretta, A., Cereti, A., Menghini, A., Annunziatellis, A., Ciotoli, G., Beaubien, S.E., Lombardi, S., 2004. GPR and EM31 investigations on an active CO2 gas vent. In: Tenth International Conference on Ground Penetrating Radar, Delft, The Netherlands, June 21–24.
Pettinelli, E., Beaubien, S.E., Lombardi, S., Annan, A.P., 2008. GPR, TDR, and geochemistry measurements above an active gas vent to study near-surface gas-migration pathways. Geophysics 73 (1), A11–A15, doi:10.1190/1.2815991.
Pfanz, H., Vodnik, D., Wittmann, C., Aschan, G., Batic, F., Turk, B., Macek, I., 2007. Photosynthetic performance (CO2compensation point, carboxylation efficiency, and net photosynthesis) of timothy grass

(Phleum pratense L.) is affected by elevated carbon dioxide in post-volcanic mofette areas. Env. Exp. Bot. 61, 41–48.

Rillig, M.C., Hernandez, G.Y., Newton, P.C.D., 2000. Arbuscular mycorrhizae respond to elevated atmospheric CO2 after long-term exposure: evidence from a CO2 spring in New Zealand supports the resource balance model. Ecol. Lett. 3 (6), 475–478, doi:10.1046/j.1461-0248.2000.00178.x.

Robredo, A., Perez-Lopez, U., Sainz de la Maza, H., Gonzalez-Moro, B., Lacuesta, M., Mena-Pete, A., Munoz-Rueda, A., 2007. Elevated CO2 alleviates the impact of drought on barley improving water status by lowering stomatal conductance and delaying it effects on photosynthesis. Env. Exp. Bot. 59, 252–263.

Ross, D.J., Tate, K.R., Newton, P.C.D., Wilde, R.H., Clark, H., 2000. Carbon and nitrogen pools and mineralization in a grassland gley soil under elevated carbon dioxide at a natural CO2 spring. Global Change Biol. 6, 779–790.

Selvi, F., 1997. Acidophilic grass communities of CO2-springs in central Italy: composition, structure, and ecology. In: Raschi, A., Miglietta, F., Tognetti, R., van Gardingen, P.R. (Eds.), Plant Responses to Elevated CO2: Evidence from Natural Springs. Cambridge University Press, Cambridge.

Stephens, J.C., Hering, J.G., 2002. Comparative characterization of volcanic ash soils exposed to decade-long elevated carbon dioxide concentrations at Mammoth Mountain, California. Chem. Geol. 186, 301–313.

Stephens, J.C., Hering, J.G., 2004. Factors affecting the dissolution kinetics of volcanic ash soils: dependencies on pH, CO2, and oxalate. Appl. Geochem. 19 (8), 1217–1232.

Stock, W.D., Ludwig, F., Morrow, C., Midgley, G.F., Wand, S.J.E., Allsopp, N., Bell, T.L., 2005. Long-term effects of elevated atmospheric CO2 on species composition and productivity of a southern African C4 dominated grassland in the vicinity of a CO2 exhalation. Plant Ecol. 178, 211–224.

Teng, F., Tondeur, D., 2007. Efficiency of carbon storage with leakage: physical and economical approaches. Energy 32, 540–548.

Tognetti, R., Cherubini, P., Innes, J.L., 2000. Comparative stem-growth rates of Mediterranean trees under background and naturally enhanced ambient CO2 concentrations. New Phytol. 146 (1), 59–74, doi:10.1046/j.1469-8137.2000.00620.x.

Vessey, J.K., Pawlowski, K., Bergman, B., 2005. Root-based N2fixing symbioses: legumes, actinorhizal plants, Parasponia sp. and cycads. Plant Soil 274 (1–2), 51–78.

Vezzoli, L., Conticelli, S., Innocenti, F., Landi, P., Manetti, P., Palladino, D.M., Trigila, R., 1987. Stratigraphy of the Latera volcanic complex: proposals for a new nomenclature. Per. Miner. 56, 89–110.

Vodnik, D., Kastelec, D., Pfanz, H., Macek, I.B.T., 2006. Small-scale spatial variation in soil CO2 concentration in a natural carbon dioxide spring and some related plant responses. Geoderma 133, 309–319.

West, J.M., Pearce, J.M., Bentham, M., Maul, P., 2005. Environmental issues and the geological storage of CO2. Eur. Env. 15, 250–259.

West, J.M., Pearce, J.M., Bentham, M., Rochelle, C., Maul, P., Lombardi, S., 2006. Environmental issues and the geological storage of CO2—a European perspective. In: 8th International Conference on Greenhouse Gas Control Technologies, Trondheim, Norway, June 19–22.

White, C.M., Strazisar, B.R., Granite, E.J., Hoffman, J.S., Pennline, H.W., 2003. Separation and capture of CO2 from large stationary sources and sequestration in geological formations—coalbeds and deep saline aquifers. J. Air Waste Manage. Assoc. 53, 645–715.

Wilson, M., Monea, M. (Eds.), 2004. IEA GHG Weyburn CO2 Monitoring and Storage Project Summary Report 2000–2004, vol. III. Petroleum Technology Research Centre, Regina, 273 pp.

Worden, R.H., Smith, L.K., 2004. Geological sequestration of CO2 in the subsurface: lessons from CO2 injection enhanced oil recovery projects in oilfields. In: Baines, S.J., Worden, R.H. (Eds.), Geological Storage of Carbon Dioxide, vol. 233. Geological Society of London, London, Special Publications, pp. 211–224.

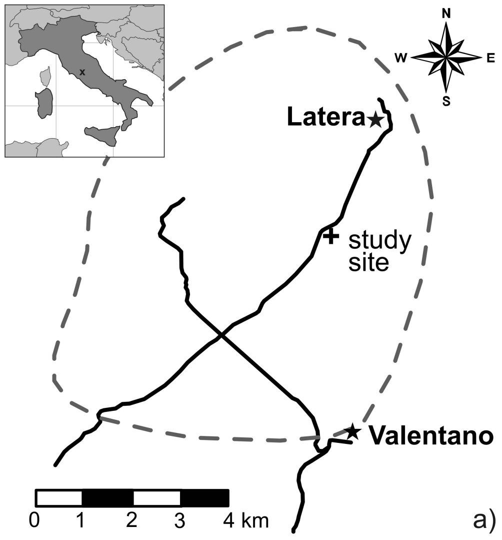
N
W
E
S
x
Latera
study site
Valentano
0
1
2
3
4 km
a)


b)

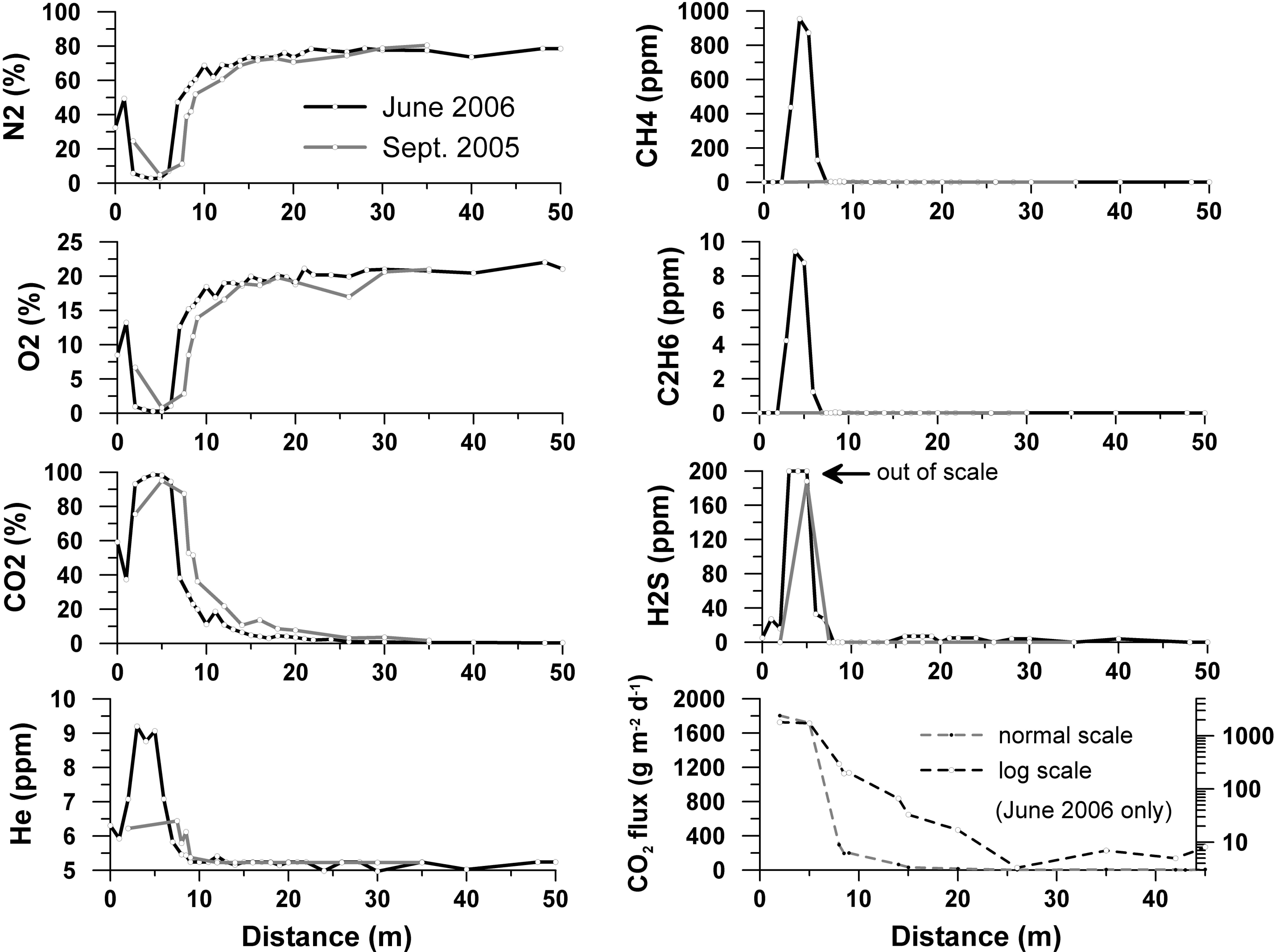
N2 (%)
June 2006
Sept. 2005
CH4 (ppm)
O2 (%)
C2H6 (ppm)
CO2 (%)
H2S (ppm)
out of scale
He (ppm)
CO$_2$ flux (g m^{-2} d^{-1})
normal scale
log scale
(June 2006 only)
Distance (m)
Distance (m)

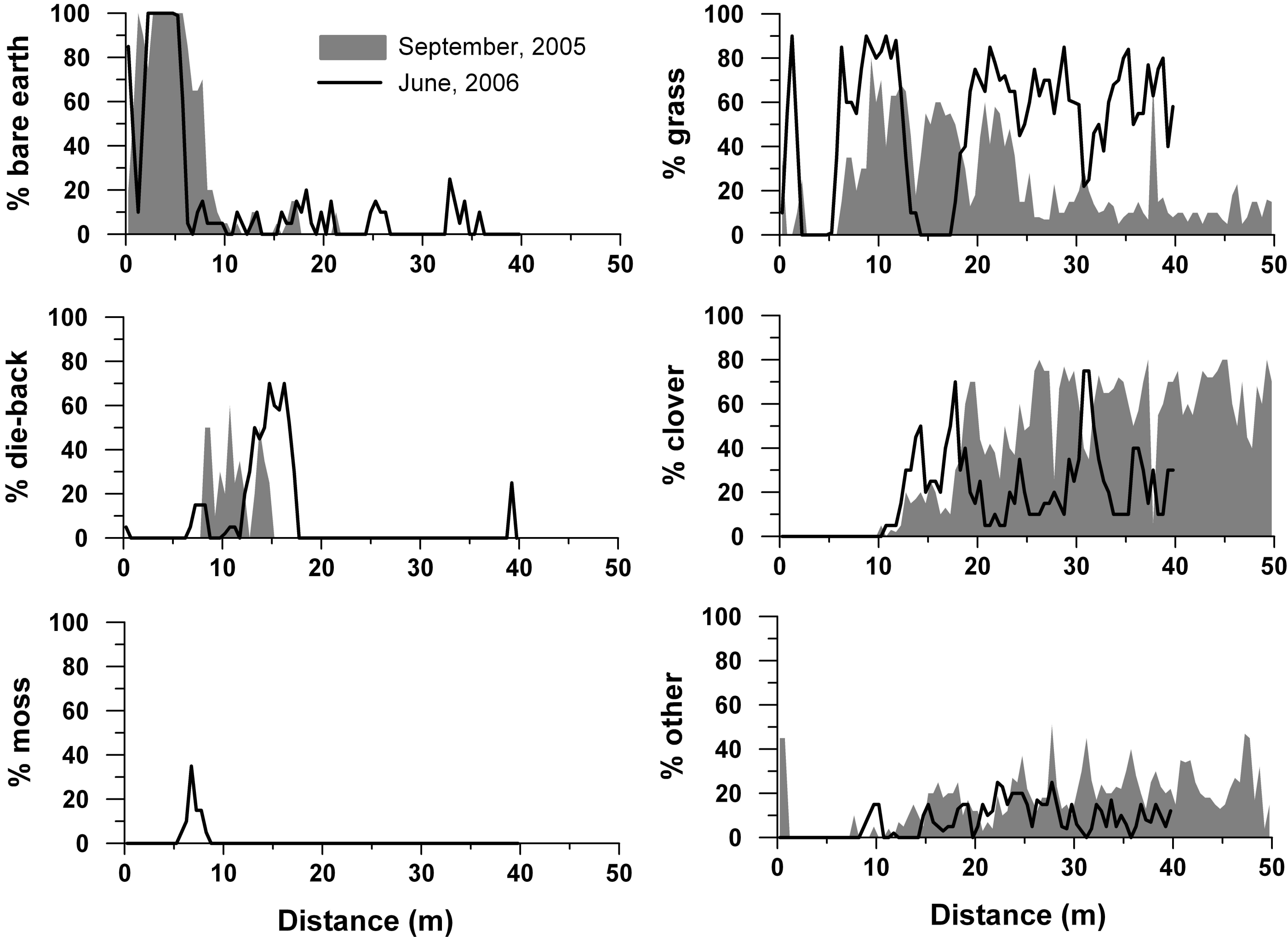
September, 2005
June, 2006
% bare earth
% grass
% die-back
% clover
% moss
% other
0
20
40
60
80
100
0
10
20
30
40
50
Distance (m)
Distance (m)

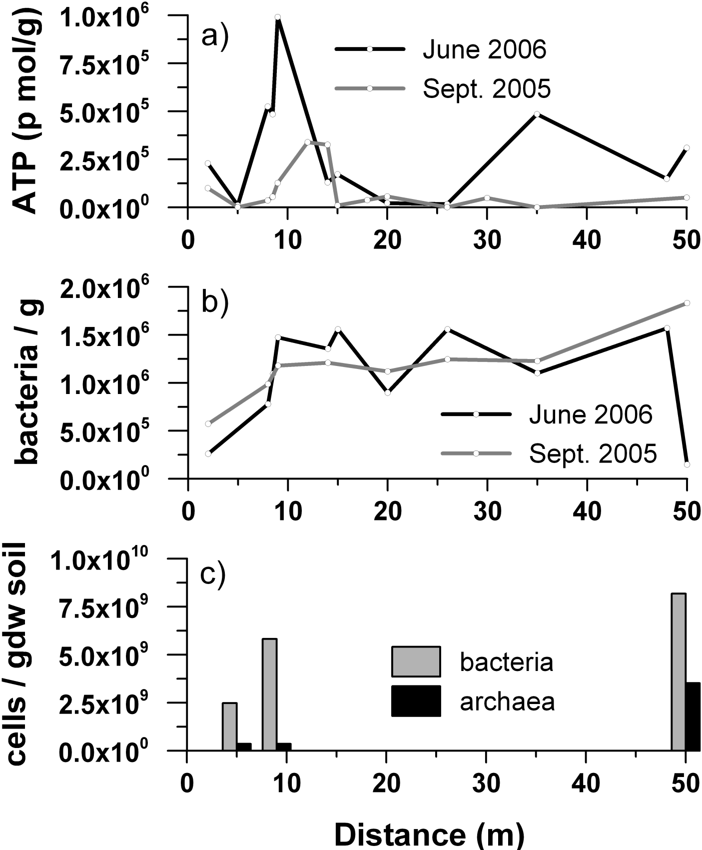
a)
June 2006
Sept. 2005
ATP (p mol/g)
1.0x10^6
7.5x10^5
5.0x10^5
2.5x10^5
0.0x10^0
0
10
20
30
40
50
b)
bacteria / g
2.0x10^6
1.5x10^6
1.0x10^6
5.0x10^5
0.0x10^0
June 2006
Sept. 2005
0
10
20
30
40
50
c)
cells / gdw soil
1.0x10^10
7.5x10^9
5.0x10^9
2.5x10^9
0.0x10^0
bacteria
archaea
0
10
20
30
40
50
Distance (m)

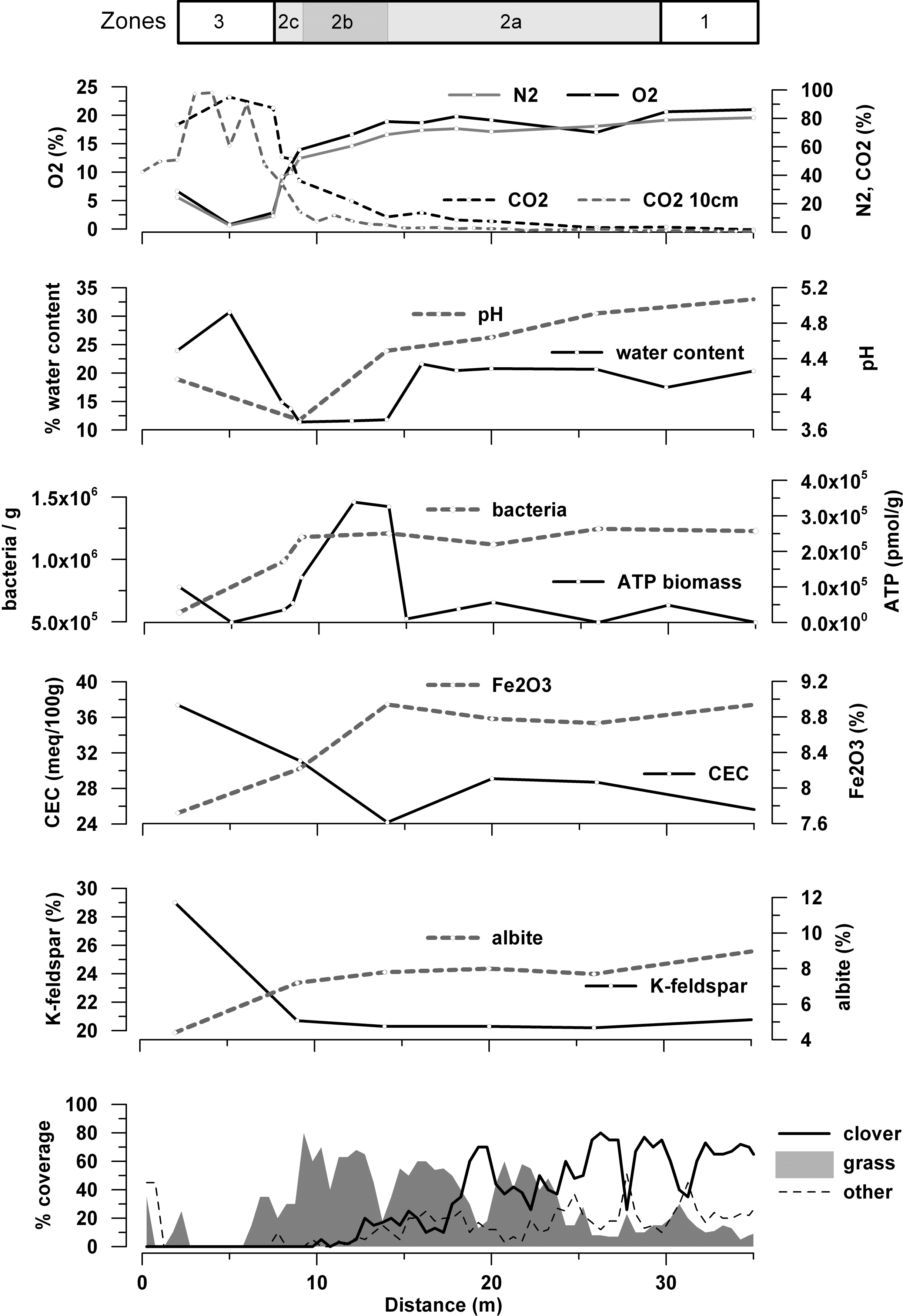
Zones
3
2c
2b
2a
1
O2 (%)
N2, CO2 (%)
N2
O2
CO2
CO2 10cm
0
5
10
15
20
25
0
20
40
60
80
100
% water content
pH
water content
10
15
20
25
30
35
3.6
4
4.4
4.8
5.2
bacteria / g
ATP (pmol/g)
bacteria
ATP biomass
$5.0x10^5$
$1.0x10^6$
$1.5x10^6$
$0.0x10^0$
$1.0x10^5$
$2.0x10^5$
$3.0x10^5$
$4.0x10^5$
CEC (meq/100g)
Fe2O3 (%)
Fe2O3
CEC
24
28
32
36
40
7.6
8
8.4
8.8
9.2
K-feldspar (%)
albite (%)
albite
K-feldspar
20
22
24
26
28
30
4
6
8
10
12
% coverage
clover
grass
other
0
20
40
60
80
100
0
10
20
30
Distance (m)

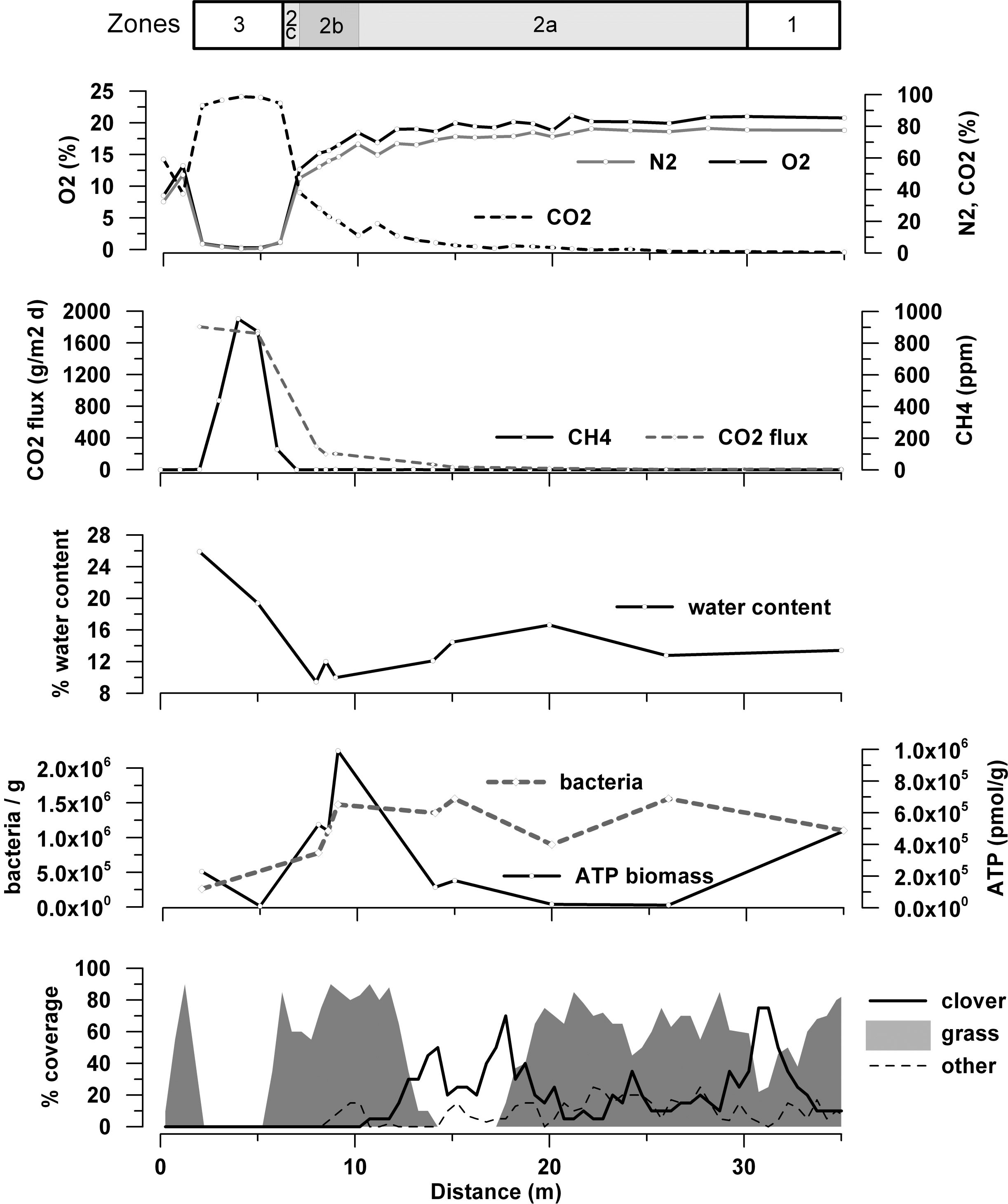
Zones
3
2c
2b
2a
1
O2 (%)
N2, CO2 (%)
N2
O2
CO2
CO2 flux (g/m2 d)
CH4 (ppm)
CH4
CO2 flux
% water content
water content
bacteria / g
ATP (pmol/g)
bacteria
ATP biomass
% coverage
clover
grass
other
Distance (m)
0
10
20
30